Follow us @BoneJointRes

Freely available online OPEN ACCESS

BJR

INFECTION

Rifampicin restores extracellular organic matrix formation and mineralization of osteoblasts after intracellular *Staphylococcus aureus* infection

F. I. Alagboso,
G. K. Mannala,
N. Walter,
D. Docheva,
C. Brochhausen,
V. Alt,
M. Rupp

From University Hospital Regensburg, Regensburg, Germany

Aims

Bone regeneration during treatment of staphylococcal bone infection is challenging due to the ability of *Staphylococcus aureus* to invade and persist within osteoblasts. Here, we sought to determine whether the metabolic and extracellular organic matrix formation and mineralization ability of *S. aureus*-infected human osteoblasts can be restored after rifampicin (RMP) therapy.

Methods

The human osteoblast-like Saos-2 cells infected with *S. aureus* EDCC 5055 strain and treated with 8 µg/ml RMP underwent osteogenic stimulation for up to 21 days. Test groups were Saos-2 cells + *S. aureus* and Saos-2 cells + *S. aureus* + 8 µg/ml RMP, and control groups were uninfected untreated Saos-2 cells and uninfected Saos-2 cells + 8 µg/ml RMP.

Results

The *S. aureus*-infected osteoblasts showed a significant number of intracellular bacteria colonies and an unusual higher metabolic activity ($p < 0.005$) compared to uninfected osteoblasts. Treatment with 8 µg/ml RMP significantly eradicated intracellular bacteria and the metabolic activity was comparable to uninfected groups. The RMP-treated infected osteoblasts revealed a significantly reduced amount of mineralized extracellular matrix (ECM) at seven days osteogenesis relative to uninfected untreated osteoblasts ($p = 0.007$). Prolonged osteogenesis and RMP treatment at 21 days significantly improved the ECM mineralization level. Ultrastructural images of the mineralized RMP-treated infected osteoblasts revealed viable osteoblasts and densely distributed calcium crystal deposits within the extracellular organic matrix. The expression levels of prominent bone formation genes were comparable to the RMP-treated uninfected osteoblasts.

Conclusion

Intracellular *S. aureus* infection impaired osteoblast metabolism and function. However, treatment with low dosage of RMP eradicated the intracellular *S. aureus*, enabling extracellular organic matrix formation and mineralization of osteoblasts at later stage.

Cite this article: *Bone Joint Res* 2022;11(5):327–341.

Keywords: *Staphylococcus aureus*, Osteoblast, Metabolism, Mineralization, Rifampicin

Article focus

- The bone regeneration competence of *Staphylococcus aureus*-infected human osteoblasts after effective rifampicin (RMP) therapy.
- The therapeutic effect of intracellular penetrative antibiotic for the eradication of bacteria within osteoblasts.

Key messages

- Intracellular *S. aureus* infection significantly impairs osteoblast metabolism and function.
- Metabolic and bone formation activities of osteoblasts can be restored in staphylococcal related bone disease after successful eradication of intracellular bacteria.

Correspondence should be sent to Markus Rupp; email: Markus.rupp@ukr.de

doi: 10.1302/2046-3758.115.BJR-2021-0395.R1

Bone Joint Res 2022;11(5):327–341.

- RMP is a potent intracellular penetrating antibiotic effective in the eradication of intracellular bacteria at reduced concentration.

Strengths and limitations

- By employing different analytical methods, this in vitro study showed that the metabolic and bone formation activities of infected human osteoblasts can be restored after successful treatment with an intracellular penetrating antibiotic.
- This study requires validation in both in vivo and clinical studies.

Introduction

Osteomyelitis is a debilitating bone disease caused by bacterial and fungal pathogens, which affects quality of life and is thus a huge burden on the public health system. Osteomyelitis can arise because of haematogenous infection or implant-associated bone infection. Therefore, an oncology-based system was recently proposed to classify periprosthetic joint infections (PJIs) to improve patients' clinical outcomes. This PJI-TNM system assesses the local situation of the tissue and the indwelling implant (T), causative non-human bacterial and/or fungal organisms (N), and the morbidity of the patient (M). Based on the score, the PJI-TNM system provides guidelines to treat the patients and improve their clinical outcome.[1,2]

S. aureus is a well-known gram-positive bacterium responsible for a large proportion of osteomyelitis cases. The infections start with binding of the bacteria to the host proteins such as fibrinogen found on the prosthesis, to form the sessile mode of growth on the implant called biofilms. Once biofilms are formed, the bacteria are able to evade the host immune system and become more resistant to antibiotic treatment.[3,4] In addition to biofilm formation on implants, these bacteria can spread into bone matrix and the bone cells, causing inflammation and thereby interfering with the normal bone healing process.[5-7] Currently, new methods are being tested for treatment of biofilm-associated bone infection, namely the use of bone cement loaded with circulating drugs,[8] use of shockwaves,[9] and heat induction in combination with antibiotics.[10]

Previously, *S. aureus* was considered an extracellular pathogen. However, recent findings have shown that *S. aureus* is also a facultative intracellular pathogen that is capable of invading and surviving inside eukaryotic cells, including specialized phagocytes such as neutrophils and macrophages and amateur phagocytes such as fibroblasts and osteoblasts.[11-13] Moreover, *S. aureus* is also able to migrate and proliferate in the host lacunar–canaliculi network, which serves as a reservoir for chronic infections.[14,15] In recent years, it has also become evident from in vitro and in vivo studies that *S. aureus* is capable of invading other bone cells such as osteoblasts, osteoclasts, and osteocytes, where it proliferates and enters into dormant stage leading to a persistent infection.[16-18] The invasion of *S. aureus* within osteoblasts is a key virulence factor to escape antimicrobial therapy and to evade host immune response leading to prolonged survival, thereby promoting incessant infection.[19-22] The capability of *S. aureus* to internalize osteoblasts is linked to its ability to directly bind many bone extracellular matrix (ECM) components, such as fibronectin, collagen, and bone sialoprotein via a special group of adhesins called the microbial surface components, which recognize adhesive matrix molecules.[23-26] Moreover, *S. aureus* can directly interact with specific receptors on osteoblasts such as tumour necrosis factor receptor through its staphylococcal protein A (SpA).[27] Once internalized, *S. aureus* can persist inside osteoblasts by localizing in endocytic vesicular bodies or transforming into quasi-dormant small colony variants.[12,28]

Osteoblasts are major directors of bone regeneration following normal physiological turnover and pathological incidents. The persistence of *S. aureus* as an intracellular pathogen in osteomyelitis leads to substantially increased osteoblast death.[29,30] Also, the viability and activity of surviving osteoblasts are impaired by the bacteria burden. Several in vitro *S. aureus* infection models reported decreased osteoblast proliferation, differentiation, and matrix mineralization in infected osteoblasts.[31,32] The reduction in number and activity of surviving osteoblasts negatively impacts bone formation and promotes bone resorption. The imbalance between the osteoblasts and osteoclasts provokes serious alterations in the bone remodelling process that affect the inflammatory cytokine milieu, especially the receptor activator of NF-$_k$B ligand (RANKL) and osteoprotegerin (OPG). RANKL and OPG produced by osteoblasts are the key promotor and inhibitor, respectively, of osteoclastogenesis during bone remodelling.[33,34] *S. aureus* infection of osteoblasts is associated with an increase in RANKL and a decrease in OPG gene expression, and thus favours osteoclast differentiation and activation with subsequent osteolysis and bone loss.[35,36]

Rifampicin (RMP), an ansamycin, is highly efficient in eradicating intracellular *S. aureus*, especially at reduced clinical concentrations when compared to other antibiotic agents such as gentamicin (GEN), vancomycin, daptomycin, ofloxacin, or tigecycline.[32,37,38] However, it remains unknown whether the metabolic and bone regeneration capabilities of *S. aureus*-infected human osteoblasts can be restored after successful eradication of intracellular bacteria burden.

Therefore, this study aims to evaluate the metabolic, organic matrix formation and mineralization competence of human osteoblast-like Saos-2 cells after eradication of intracellular *S. aureus* using RMP as the antimicrobial agent.

Methods

Bacteria culture. The *S. aureus* EDCC 5055 bacteria strain as described by Alt et al,[39] a clinical isolate from a patient

Table I. Real-time polymerase chain reaction primer sequences.

RefSeq accession ID	Full gene name	Gene	Forward primer sequence 5' → 3'	Reverse primer sequence 5' → 3'
NM_001177520.3	Alkaline phosphatase, biomineralization associated	*ALPL*	ACCACCACGAGAGTGAACCA	CGTTGTCTGAGTACCAGTCCC
NM_199173.6	Bone gamma-carboxyglutamate protein / Osteocalcin	*BGLAP*	GAAGCCCAGCGGTGCA	CACTACCTCGCTGCCCTCC
NM_001200.4	Bone morphogenic protein type 2	*BMP2*	AACACTGTGCGCAGCTTCC	CTCCGGGTTGTTTTCCCAC
NM_000088.4	Collagen type 1	*COL1A1*	ACGTCCTGGTGAAGTTGGTC	ACCAGGGAAGCCTCTCTCTC
NM_000194.3	Hypoxanthine phosphoribosyltransferase 1	*HPRT1*	CGAGATGTGATGAAGGAGATGG	GCAGGTCAGCAAAGAATTTATAGC
NM_002546.4	Tumour necrosis factor (TNF) receptor super-family member 11b / Osteoprotegerin	*OPG*	GCTCACAAGAACAGACTTTCCAG	CTGTTTTCACAGAGGTCAATATCTT
NM_003701.4	Receptor activator of NF-κB ligand	*RANKL*	CATCCCATCTGGTTCCCATAA	GCCCAACCCCGATCATG
NM_001015051.3	Runt-related transcription factor 2	*RUNX2*	ATACCGAGTGACTTTAGGGATGC	AGTGAGGGTGGAGGGAAGAAG
NM_003118.4	Secreted protein acidic and rich in cysteine	*SPARC*	ATCTTCCCTGTACACTGGCAGTTC	CTCGGTGTGGGAGAGGTACC

with wound infection that shows strong haemolytic and biofilm formation ability, was used for this study. The *S. aureus* EDCC 5055 strain is cultured in brain heart infusion (BHI) broth. The bacteria culture was inoculated in the BHI broth and incubated at 37°C for six to eight hours.

In vitro bacterial infection of human osteoblast-like Saos-2 cells. The in vitro infection model was established using the early passage of human osteoblast-like Saos-2 cell line. The cells were grown in modified McCoy's 5A medium (Thermo Fisher Scientific, USA) supplemented with 10% fetal calf serum at 37°C in a humidified atmosphere of 4% CO_2. For the infection experiment, $2 \times 10^4/cm^2$ cells were seeded in 24-well plates and incubated at 37°C for about two to three days to reach semi-confluence. A fresh subculture of *S. aureus* EDCC 5055 strain was prepared from an overnight culture at a dilution of 1:100 and incubated for three hours with constant shaking at 180 rpm until it reached exponential growth phase. Next, the optical density of the bacteria subculture was diluted to 1 at 600 nm using a spectrophotometer. Then, the bacteria culture was resuspended in fresh McCoy's 5A medium, and the cells were infected at a multiplicity of infection (MOI) 30. Thereafter, the cells were incubated for 30 minutes at 37°C to allow bacteria invasion. Thereafter, the supernatant was discarded, and the cell monolayer was washed two times with phosphate buffered saline (PBS). Then, cells were incubated in medium containing 30 µg/ml GEN at 37°C for 30 minutes to kill the extracellular bacteria.[32] Subsequently, cells were washed two times in PBS to remove dead bacteria and cell debris.

Immunofluorescence staining. To visualize the intracellular bacteria, Saos-2 cells were cultivated onto glass slides and infected with *S. aureus* EDCC 5055 as described above. After three hours of incubation, the supernatant was removed and slides were washed two times with PBS. Thereafter, the cells were fixed with 10% paraformaldehyde for 15 minutes at room temperature and subsequently washed three times with PBS. The cells were permeabilized with 0.2% (v/v) Triton X-100 in PBS for 30 minutes. After two hours of incubation in 3% bovine serum albumin, the slides were incubated with anti-*S. aureus* rabbit polyclonal antibody (Bio-Rad, USA) at a dilution of 1:300 overnight at 4°C. Primary antibody was detected with Cy3-conjugated goat anti-rabbit secondary antibody (Jackson Immuno-Research, USA) at dilution of 1:200 for one hour at room temperature. Thereafter, F-actin filaments were stained with phalloidin-iFluor 488 (Abcam, UK) for 60 minutes, followed by nuclei counterstaining with DAPI for ten minutes. The slides were examined using a fluorescence microscope (Zeiss, Germany), and images were captured with an integrated camera equipped with ZEN 3.0 software.

Transmission electron microscopy. To characterize the ultrastructure of *S. aureus*-infected osteoblasts, Saos-2 cells were seeded onto Thermanox plastic coverslips (Nalge Nunc International, USA) inserted in a 24-well plate. After three hours of infection, the culture medium was discarded, and cells were washed two times with PBS. Subsequently, the cells were fixed with Karnovsky fixatives (0.1 M cacodylate buffer with 2.5% glutaraldehyde and 2% paraformaldehyde). The cells were fixed again with 1% osmium tetroxide at pH 7.3 and dehydrated through a graded series of ethanol. Next, the samples were embedded in EMbed-812 epoxy resin (Science Services, Germany) and polymerized at 60°C for 48 hours. Prior to cutting, the plastic coverslips were removed from the Epon blocks and the samples were cut into semi-thin sections of 0.75 µm thickness. Sections were stained with toluidine blue and basic fuchsine solution and visualized using a light microscope to localize regions of interest for ultrastructural analysis. Subsequently, ultra-thin sections of about 80 nm thickness were cut using a Reichert Ultracut-S ultramicrotome (Leica, Germany) equipped with a diamond knife (DU3525; Diatome, Switzerland). Sections were mounted on grids and contrasted with aqueous 2% uranyl acetate and lead citrate solution for ten minutes each. Finally, the sections were analyzed with a LEO912AB transmission electron microscope (Zeiss, Germany) operating at 100 kV. High-resolution images were acquired with an integrated Sharp Eye 2 k slow-scan CCD camera (TRS, Germany).

Resazurin for RMP cytotoxicity assay and assessment of metabolic activity of the infected Saos-2 cells pre- and

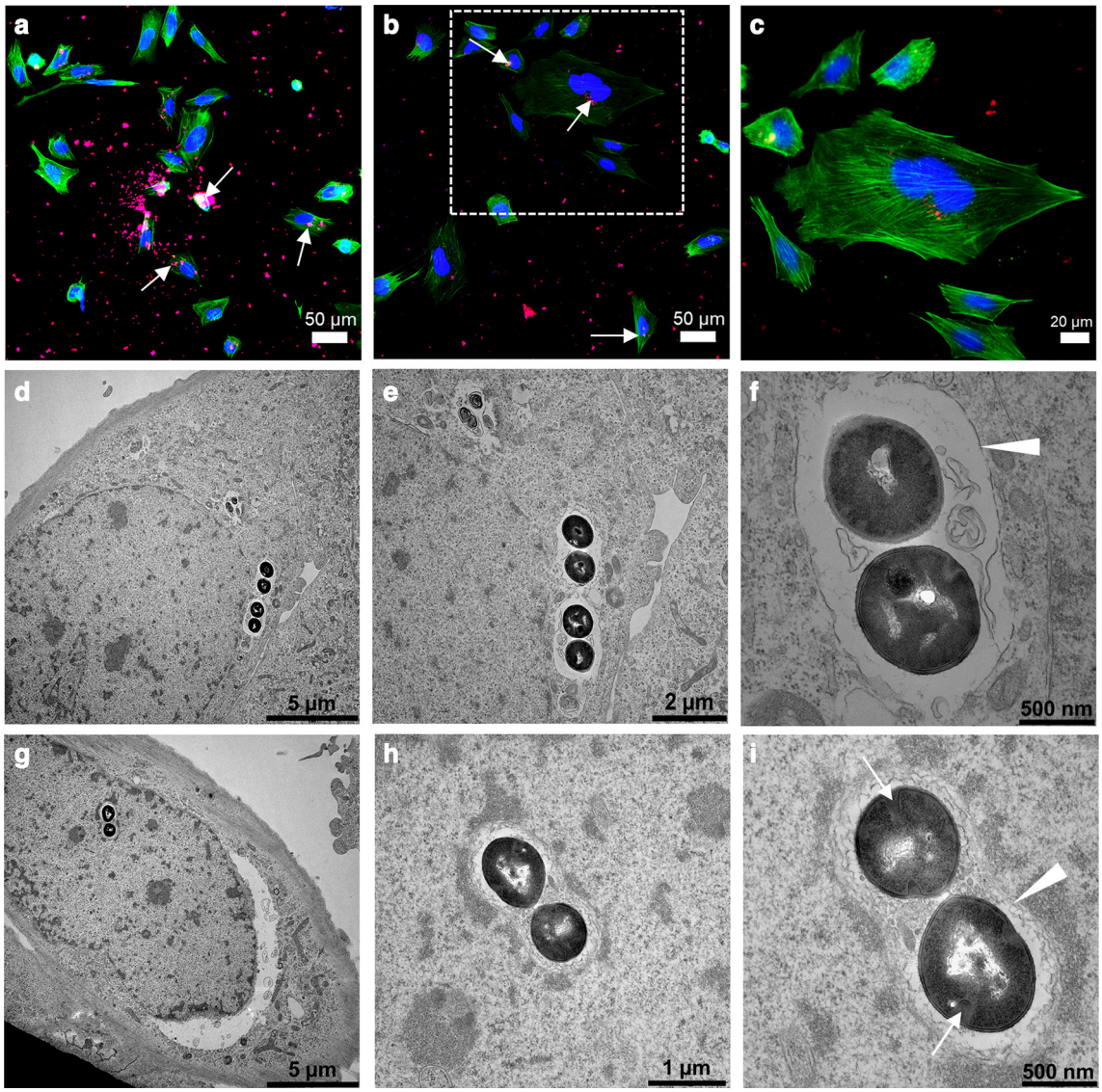

Fig. 1

Intracellular invasion of *Staphylococcus aureus* in osteoblasts. a) to c) Immunofluorescence images showing clusters of *S. aureus* EDCC 5055 that are localized inside the Saos-2 cells at three hours post-infection. The *S. aureus* (white arrows), nuclei, and actin filament are stained in red, blue, and green, respectively. d) to i) Ultrastructural imaging of intracellular *S. aureus* EDCC 5055 revealed internalized bacteria clusters localized close to the cell nuclei membrane. Most bacteria clusters possess intact cell wall/plasma membrane and are surrounded by phagosomal membrane (white arrowheads). Some proliferating bacteria revealed division septa (white arrows).

post-antibiotic treatment. First, the cytotoxic effect of RMP on Saos-2 cell metabolism was determined using the resazurin assay. Briefly, semi-confluent Saos-2 cells seeded in 24-well plates were treated with either single or multiple doses of different concentrations of RMP, namely 0, 4, 8, 16, 50, 100, and 200 µg/ml at different timepoints. To measure the cellular metabolic activity, the cells were incubated with the non-fluorescence resazurin dye for three hours at 37°C. Resazurin is a non-fluorescent blue dye that is metabolically reduced to a strong fluorescent resorufin after reacting with viable eukaryotic and prokaryotic cells.[40,41] The fluorescence intensity of the resorufin correlates with the level of cellular metabolism in viable cells, which is then measured with a spectrophotometer (Tecan, Switzerland). Similarly, resazurin assay was used to measure the metabolic activity of the planktonic *S. aureus* culture and the *S. aureus* infected Saos-2 cells after treatment with single dose of 8 µg/ml RMP relative to the uninfected osteoblasts at days 1, 2, and 3. The mean resorufin fluorescence unit (RFU) was determined from four independent experiments.

CFU assay for the assessment of intracellular bacteria growth after RMP therapy. To determine the intracellular *S. aureus* eradication competence of RMP, the *S. aureus* infected osteoblasts as described above were treated with 8 µg/ml RMP. After two, 24, 48, and 78 hours of incubation at 37°C, the supernatant fluids were removed, and cells were washed three times with PBS and lysed with

Figure 2

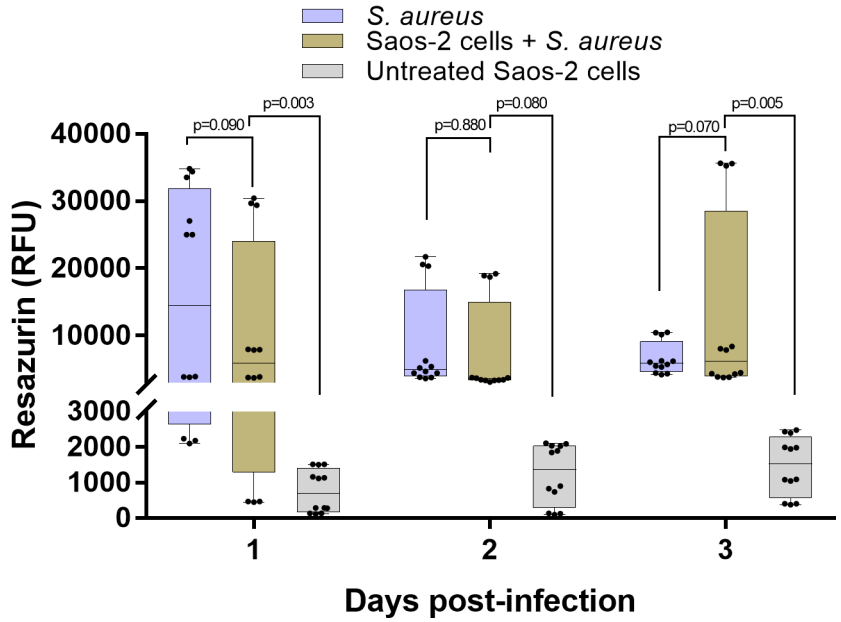

Fig. 2

Altered metabolic activity in the *Staphylococcus aureus*-infected osteoblasts. Resazurin assay of the *S. aureus*-infected osteoblasts shows abnormally high metabolic activity, similar to the planktonic bacteria, and significantly higher than the uninfected (native) osteoblasts. n = 4; two-way analysis of variance (ANOVA) with Tukey's multiple comparisons test. RFU, resorufin fluorescence unit.

0.2% Triton X-100. Subsequently, cell lysates were diluted ten times in PBS and plated onto Müller Hinton agar plate. After 16 hours of incubation at 37°C, the number of bacteria colonies was counted, and the mean intracellular colony-forming units (CFUs) were determined from three independent experiments.

Osteogenic stimulation, Alizarin red staining and quantification assay, and extracellular ALP activity measurement. To determine the osteogenic competence of Saos-2 cells infected with *S. aureus* EDCC 5055 after multiple RMP treatment, the cells were cultured in osteogenic stimulation medium containing Dulbecco's Modified Eagle Medium (DMEM) with high glucose (Thermo Fisher Scientific, USA) supplemented with 10% inactivated fetal calf serum, 100 nM dexamethasone, 10 mM β-glycerol phosphate, 50 µM L-Ascorbic acid, and 8 µg/ml RMP. The culture media were changed every two days and the matrix mineralization level was determined after seven, 14, and 21 days of osteogenic stimulation. The cell culture supernatant was collected for extracellular alkaline phosphatase (ALP) activity measurement.[42]

For the Alizarin red staining, cells were fixed with 10% paraformaldehyde for 15 minutes, washed two times with distilled water, and incubated with 40 mM Alizarin red staining solution for 45 minutes at room temperature with gentle shaking. For qualitative analysis, cells were washed three times with distilled water and images were taken using a light microscope.

Subsequently, the amount of the Alizarin red stain was quantified by extracting the dye from the cells via incubation in 10% acetic acid with gentle shaking at room temperature for 30 minutes. Next, the cell monolayer was gently scrapped, and the solution was transferred into a microcentrifuge tube and vortexed for 30 seconds. The solution was heated at 85°C for ten minutes and the slurry was centrifuged at 20,000 xg for five minutes. The supernatant was collected into a new microcentrifuge tube and neutralized with 10% ammonium hydroxide to a pH of 4.2 to 4.3. Thereafter, the optical density (OD) was measured at 405 nm along with known standard solutions.

For extracellular ALP activity measurement, 200 µl of the culture supernatant was transferred into V-bottomed 96-well plate and centrifuged for five minutes. Thereafter, 100 µl of the supernatants were transferred into a new flat-bottomed 96-well plate, and 2 mg/ml of alkaline phosphate substrate solution was added to each well. The kinetic absorbance of 35 cycles at five-minute intervals was measured at 405 nm using a spectrophotometer (Tecan, Switzerland).

RNA isolation, cDNA synthesis, and quantitative real-time PCR for gene expression analysis. Total RNA from uninfected and *S. aureus*-infected Saos-2 cells treated with 8 µg/ml RMP at various timepoints was isolated using QIAzol and RNAeasy Plus Universal Kit (Qiagen, Germany). The *S. aureus*-infected osteoblasts (Saos-2 + *S. aureus*) group was excluded from analysis due to lack of RNA. After washing with PBS, QIAzol lysis was performed on cells per 24 wells and three wells were pooled. For complementary DNA (cDNA) synthesis, 250 to 500 ng total RNA and Transcriptor First Strand cDNA Synthesis

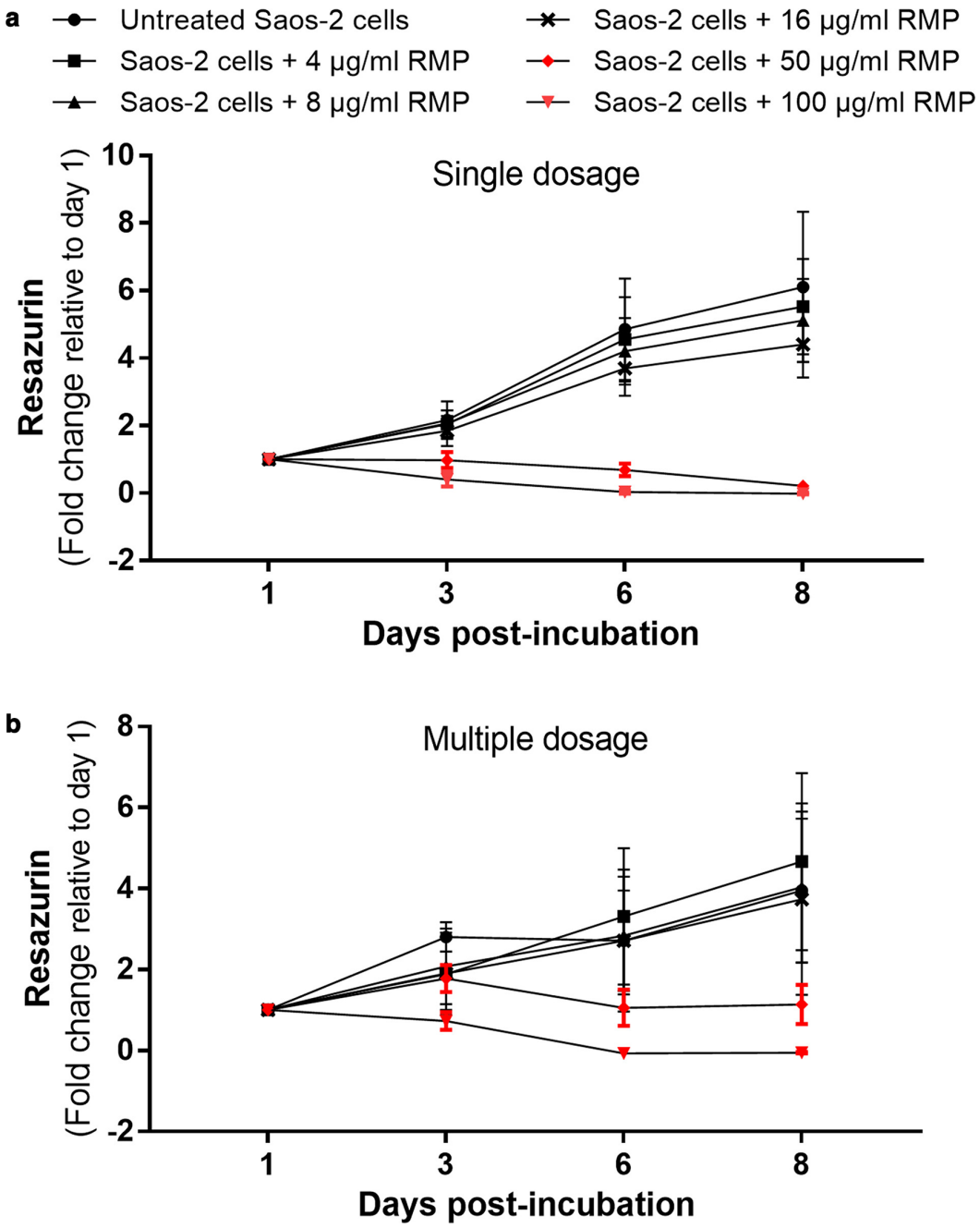

Fig. 3

Dose-dependent effect of rifampicin (RMP) on cellular metabolism. Neither a) single not b) multiple doses of < 16 mg/ml of RMP had any major adverse effect on cellular metabolism. Higher concentrations (≥ 50 µg/ml) of both single and multiple doses adversely influenced cellular proliferation and metabolism. n = 3; two-way analysis of variance (ANOVA) with Dunnett's multiple comparisons test. $p < 0.001$ at multiple dosage.

Kit (Roche, Switzerland) were used. cDNA was diluted 1:5 and quantitative real-time polymerase chain reaction (qRT-PCR) was conducted in the C1000 Touch thermocycler and CFX96 Real-Time System (Bio-Rad, Germany) at an annealing temperature of 60°C in a total volume of 20 µl using 1 µl cDNA and the Brilliant II SYBR Green QPCR Master Mix (Agilent Technologies, USA). The human gene-specific forward and reverse primers with optimal amplification efficiency are summarized in Table I.

For data analysis, raw cycle thresholds (Cts) were normalized to hypoxanthine-guanine phosphoribosyltransferase 1 (*HPRT1*) reference gene ($\Delta Ct = Ct_{target} - Ct_{reference}$). Fold induction to the correlating uninfected control 'Saos-2 cells + RMP' (mean of experimental replicates) was calculated using the $2^{-\Delta\Delta Ct}$ method with $\Delta\Delta Ct = \Delta Ct_{experimental} - \Delta Ct_{control}$.

Statistical analysis. Data analysis and graphical presentations were carried out using GraphPad Prism 7.0

Figure 4

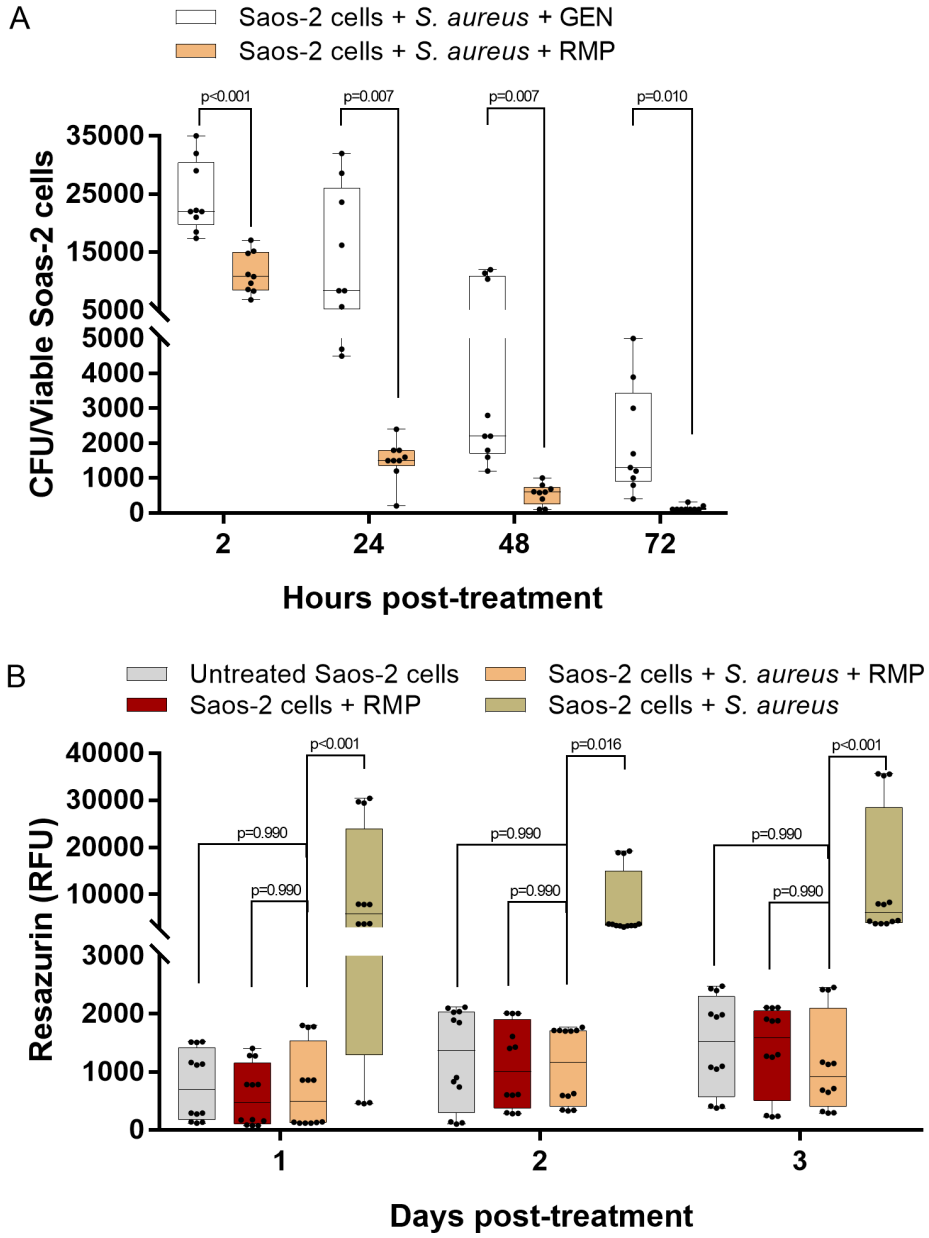

Fig. 4

High efficacy of rifampicin (RMP) in the eradication of the intracellular bacteria burden. a) Treatment of *Staphylococcus aureus*-infected osteoblasts with a single dosage of 8 µg/ml RMP substantially reduced the intracellular *S. aureus* burden as early as two hours post-treatment. Viable intracellular bacteria colony significantly decreased over time; n = 3; multiple *t*-test using the Holm-Sidak method. b) Treatment of *S. aureus*-infected osteoblasts with a single dosage of 8 µg/ml RMP enabled the restoration of host cell metabolism. The rifampicin-treated infected cells showed comparable metabolic activity to the uninfected control groups; n = 4; two-way analysis of variance (ANOVA) with Tukey's multiple comparisons test. CFU, colony-forming units; GEN, gentamicin; RFU, resorufin fluorescence unit.

(GraphPad Software, USA). Data are representative of at least three independent experiments and expressed as means (standard deviation). Significance of the represented data was calculated using two-way analysis of variance (ANOVA) for multiple comparison using Tukey's multiple comparisons test (resazurin assay, ALP assay, and quantification of osteogenesis using Alizarin red staining) and Dunnett's multiple comparisons test (cytotoxicity assay of rifampicin). Statistical significance of the treatment with GEN and rifampicin (RMP) on intracellular bacteria was determined by multiple *t*-test using the Holm-Sidak method. Statistical significance was set at $p \leq 0.05$.

Results

Intracellular invasion and proliferation of *S. aureus* in osteoblasts led to alteration of host cell metabolism. The *S.*

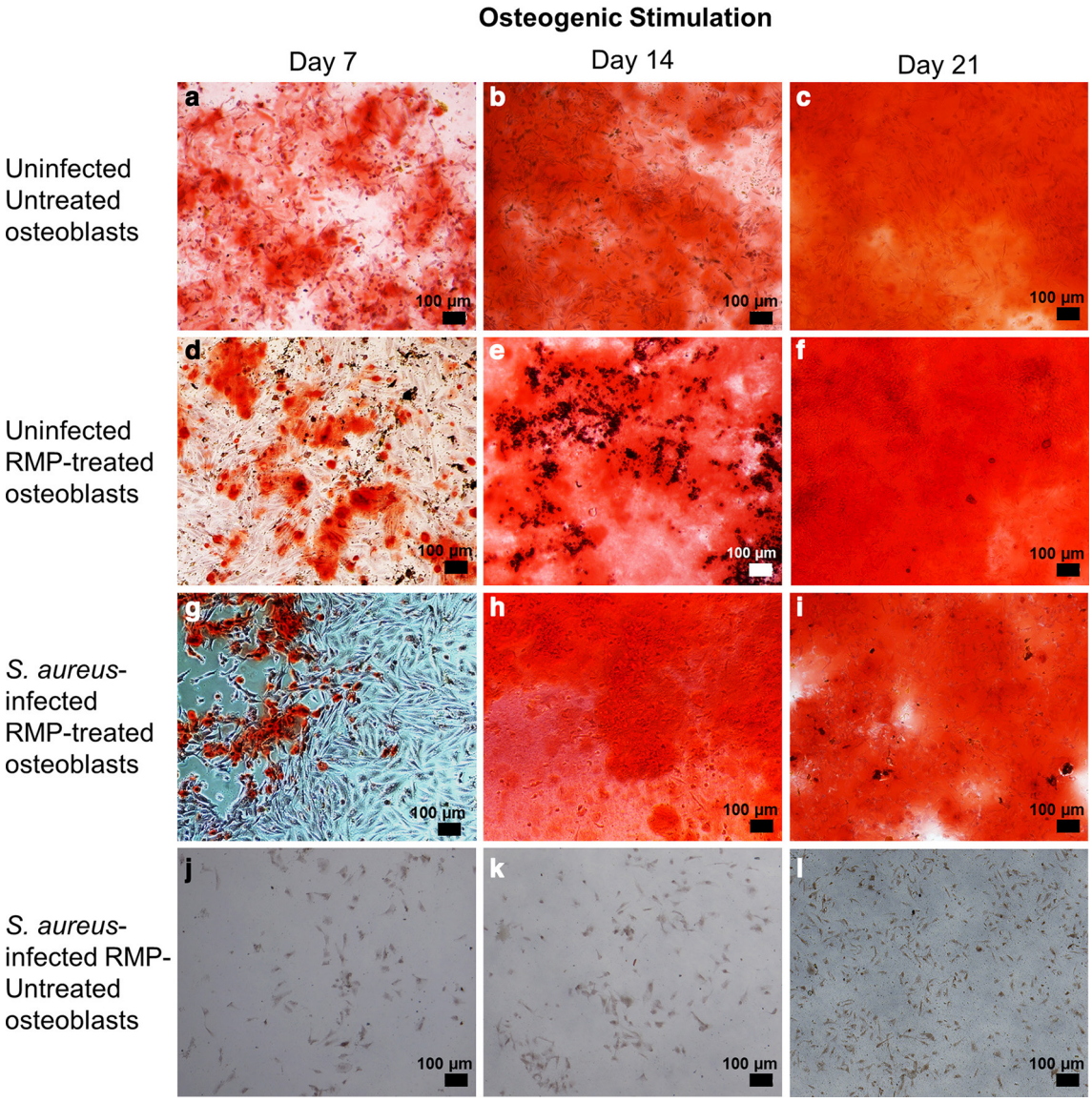

Fig. 5

The organic matrix formation and mineralization level of the rifampicin (RMP)-treated *Staphylococcus aureus*-infected osteoblasts substantially improved at later stages of osteogenesis. In comparison to the uninfected untreated (a) to c)) and uninfected RMP-treated osteoblasts (d) to f)), the RMP-treated infected osteoblasts (g) to i)) showed the least matrix mineralization at day 7 that further improved at days 14 and 21 of osteogenesis. Lack of organic matrix synthesis and mineralization is evident in the *S. aureus*-infected untreated osteoblasts (j) to l)) throughout the osteogenesis period. All of the captured images were generated after Alizarin red staining.

aureus strain EDCC 5055 efficiently invaded the Saos-2 cells after three hours post-infection. Both immunofluorescence (Figures 1a to 1c) and transmission electron microscopy (TEM) (Figures 1d to 1i) images revealed clusters of internalized bacteria that mainly localized close to the infected host cell nuclei. The ultrastructural images reveal clusters of bacteria with intact cell wall and plasma membrane. Dividing septa indicating an active proliferation stage are evident in some bacteria (Figures 1g to 1i). Furthermore, the bacteria clusters were surrounded by either complete or incomplete phagosomal membrane (Figures 1f to 1i). To determine if the intracellular bacterial infection altered the normal host cell metabolism, the metabolic activity of the *S. aureus*-infected osteoblasts was compared to the planktonic *S. aureus* culture and uninfected native osteoblasts. Remarkably, the *S. aureus*-infected osteoblasts showed comparably high metabolic activity with the planktonic *S. aureus* culture ($p = 0.090$, two-way ANOVA), whereas the uninfected native osteoblasts showed a significantly lower ($p = 0.003$, two-way ANOVA) metabolic activity after one day of infection and up to three days post-infection (Figure 2). The significantly high metabolic activity of the planktonic bacteria cells, as shown by the high RFU, indicates active bacteria

Figure 6

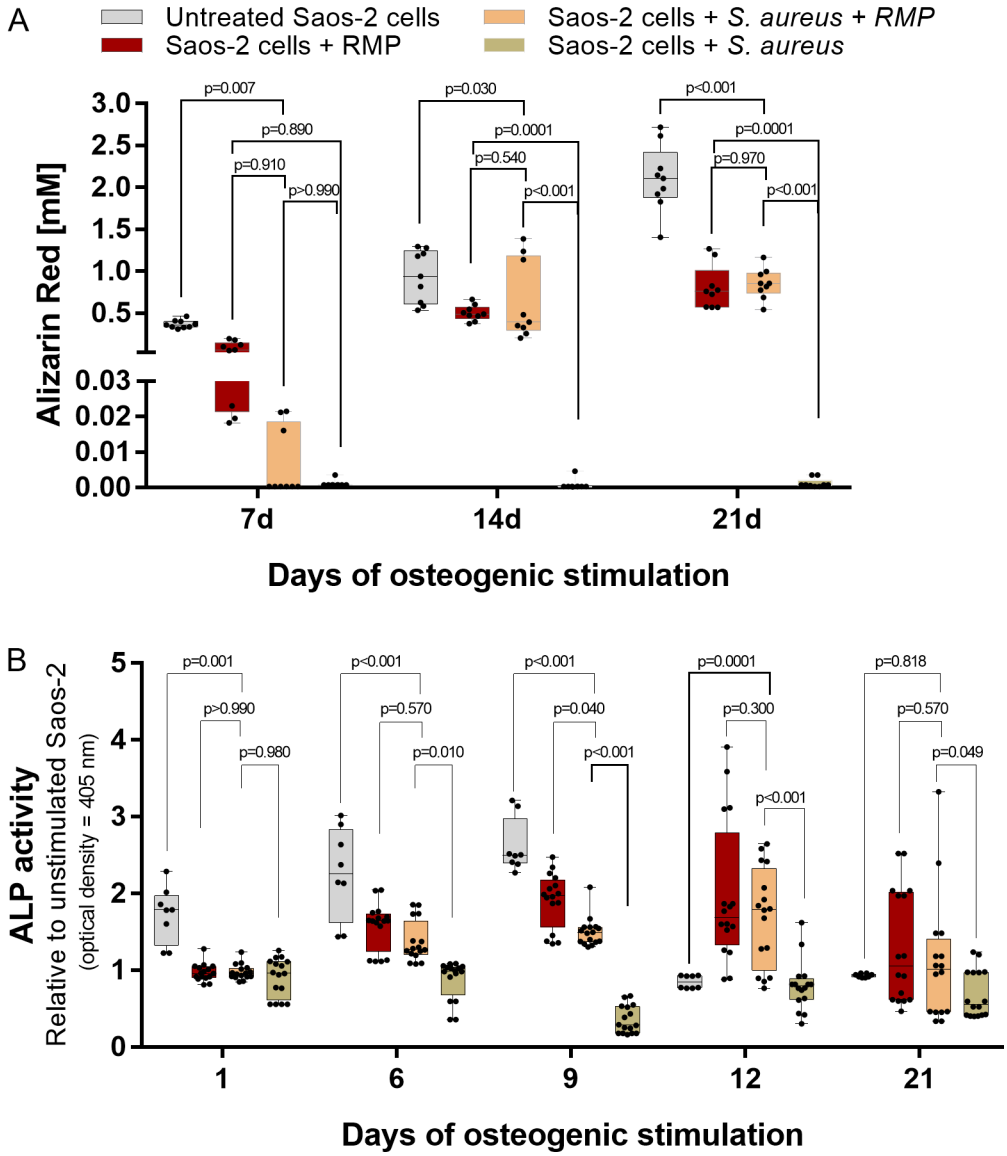

Fig. 6

a) Quantification of Alizarin red staining of the rifampicin (RMP)-treated infected osteoblasts showed the least amount of mineral deposits at day 7 that significantly improved at 14 and 21 days. b) The extracellular alkaline phosphatase (ALP) activity under osteogenesis showed an early rise in the ALP activity at days 6, 9, and 12 post-treatment, with a subsequent decrease at day 21. The *Staphylococcus aureus*-infected untreated osteoblasts showed the lowest extracellular ALP activity both at early and late osteogenesis; n = 3 to 4; two-way analysis of variance (ANOVA) with Tukey's multiple comparisons test.

proliferation, since bacteria cells are capable of metabolically reducing the non-fluorescence resazurin to a fluorescence resorufin. Similarly, active bacteria proliferation is also reflected in the high RFU of the *S. aureus*-infected osteoblasts.

Low concentration of RMP has no negative impact on cellular proliferation and metabolism. To determine the cytotoxic effect of RMP on osteoblasts, uninfected Saos-2 cells were treated with different concentrations of RMP up to eight days as either single or multiple doses. Single and multiple dosage of RMP (Figures 3a and 3b) showed that < 16 µg/ml of RMP had no significant negative impact on cellular proliferation or metabolism. However, higher concentrations (≥ 50 µg/ml) led to increased cell death with significantly reduced metabolic activity when administered as both single and multiple dosage (Figures 3a and 3b). Therefore, 8 µg/ml concentration of RMP was chosen for this study.

Single dose of 8 µg/ml of RMP significantly reduced intracellular *S. aureus* and enabled restoration of the host cell metabolism. The treatment of the *S. aureus*-infected osteoblasts with a single dose of 8 µg/ml RMP (Figure 4a) significantly reduced the intracellular bacteria burden as early as two hours post-treatment compared to the infected osteoblasts treated only with 30 µg/ml GEN ($p < 0.001$, multiple *t*-test using the Holm-Sidak method). The

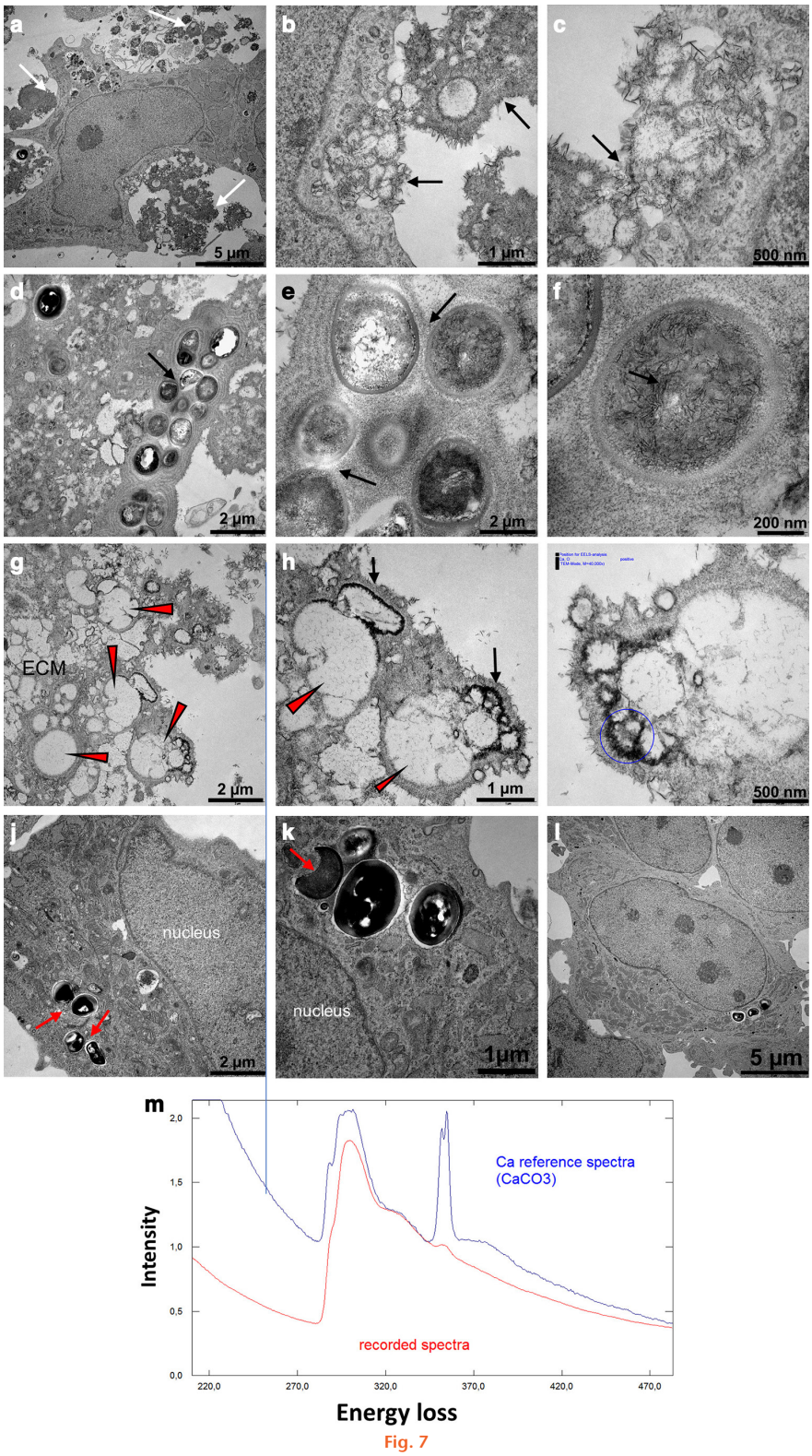

Fig. 7

Dense distribution of calcium crystal deposits within the extracellular organic matrix of the rifampicin (RMP)-treated infected osteoblasts at 21 days of osteogenesis. a) to c) The osteoblast was surrounded by a densely mineralized extracellular matrix (ECM), mostly in the form of needle-like calcium crystal deposits (white and black arrows). d) to f) The extracellular compartment revealed a colony of dead bacteria debris embedded within the densely mineralized organic matrix (black arrows), and g) to i) empty vacuoles of fully degraded bacteria (red arrowheads) were surrounded by the dense calcium crystal deposits. j) to k) The intracellular compartment revealed residual intracellular bacteria bodies with damaged microstructure (red arrows). m) The spectra lines show the reference (blue) and the recorded (red) high intensity calcium signal deposited on the ECM. There was a lack of calcium crystal deposition in the l) unstimulated RMP-treated *Staphylococcus aureus*-infected osteoblasts. All images were generated using a transmission electron microscope. CaCO3, calcium carbonate.

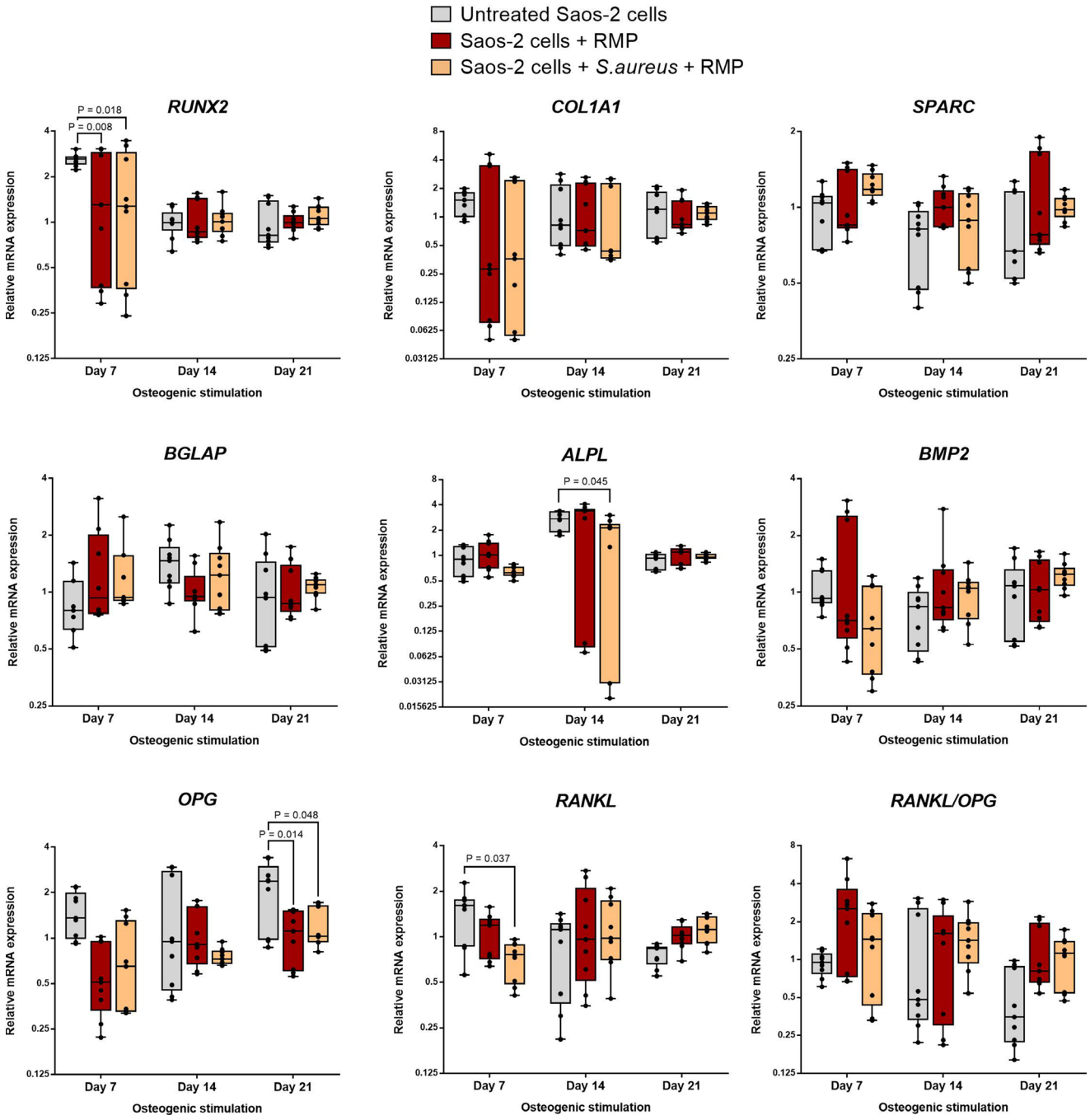

Fig. 8

Gene expression of major bone matrix formation and mineralization markers in rifampicin (RMP)-treated infected osteoblasts. In relation to the RMP-treated uninfected osteoblasts, the RMP-treated *Staphylococcus aureus*-infected osteoblasts showed a comparable gene expression level in all tested markers at days 7, 14, and 21 of osteogenic stimulation, whereas the untreated (native) uninfected osteoblasts showed significantly higher expression levels of runt-related transcription factor 2 *RUNX2* and receptor activator of NF-$_k$B ligand (*RANKL*) at day 7, and alkaline phosphatase, biomineralization associated (*ALPL*) and osteoprotegerin (*OPG*) at days 14 and 21 of osteogenesis, respectively. n = 3; two-way analysis of variance (ANOVA) with Tukey's multiple comparisons test. *BGLAP*, bone gamma-carboxyglutamate protein; *BMP2*, bone morphogenic protein 2; *COL1A*, collagen type 1 alpha 1; mRNA, messenger RNA; *SPARC*, secreted protein acidic and cysteine rich.

amount of intracellular bacteria colony was further significantly reduced after 72 hours of treatment (Figure 4a). The significant reduction of the intracellular bacteria growth using a single dose of RMP positively impacted the metabolic activity of the infected osteoblasts (Figure 4b). Interestingly, the RMP-treated *S. aureus*-infected osteoblasts showed comparable metabolic activity with the untreated (native) and RMP-treated uninfected osteoblasts ($p = 0.990$, two-way ANOVA) up to three days.

Osteoblasts produced mineralized extracellular organic matrix after eradication of intracellular *S. aureus* with RMP. To evaluate the osteogenic competence of *S. aureus*-infected osteoblasts after treatment with multiple doses of 8 µg/ml RMP, the *S. aureus*-infected osteoblasts were subjected to osteogenic stimulation. At seven days of osteogenesis, the RMP-treated infected osteoblasts (Figure 5g) produced minor quantities of mineralized extracellular organic matrix, which was significantly lower than the uninfected untreated osteoblasts ($p = 0.007$, two-way ANOVA) as shown by Alizarin red staining (Figure 5a) and quantification (Figure 6a). Furthermore, 14 and 21 days osteogenesis (Figures 5b to 5c, 5e to 5f, and 5h to 5i) led to the production of more mineralized extracellular organic matrix in an approximately 80- and 120-fold increase, respectively, compared to day 7 osteogenesis. A comparable amount of mineralization was found in the RMP-treated *S. aureus*-infected osteoblasts (Figures 5h to 5i) and RMP-treated uninfected control group (Figures 5e to 5f) at 14 ($p = 0.540$) and 21 days ($p = 0.970$, both two-way ANOVA) days osteogenesis. Also, the untreated native osteoblasts (Figures 5b to 5c) produced a significantly higher amount of mineralized matrix compared to the RMP-treated *S. aureus*-infected osteoblasts both at 14 ($p = 0.030$) and 21 ($p < 0.001$, two-way ANOVA) days osteogenesis.

To further evaluate the level of ECM mineralization, the extracellular activity of ALP was assessed directly from the cell culture supernatant (Figure 6b). The RMP-treated infected osteoblasts showed increasing ALP activity during early osteogenesis, comparable with the RMP-treated uninfected osteoblasts at six ($p = 0.570$) and 12 ($p = 0.300$, both two-way ANOVA) days. At day 21 of osteogenesis, the ALP activity of the RMP-treated *S. aureus*-infected osteoblasts decreased to a level comparable with the RMP-treated uninfected ($p = 0.570$) and untreated uninfected osteoblasts ($p = 0.818$, both two-way ANOVA).

The untreated *S. aureus*-infected osteoblasts were substantially killed and lysed by the persisting intracellular bacteria, and thus produced no form of matrix mineralization under osteogenic stimulation (Figures 5j to 5l). Similarly, their extracellular ALP activity was significantly reduced compared to the RMP-treated infected osteoblasts at day 6 ($p = 0.010$), day 9 ($p < 0.001$), day 12 ($p < 0.001$), and day 21 ($p = 0.049$, all two-way ANOVA) of osteogenesis.

Ultrastructure of the RMP-treated *S. aureus*-infected osteoblasts revealed mineralized extracellular organic matrix at 21 days of osteogenesis. The ultrastructural analysis of the RMP-treated *S. aureus*-infected osteoblasts after 21 days of osteogenic stimulation revealed osteoblasts that were surrounded by densely distributed needle-like calcium crystal deposits within the ECM (Figures 7a to 7c). The high-intensity signal of the recorded calcium spectrum confirms ECM mineralization (Figure 7m). Furthermore, the extracellular compartment of the RMP-treated *S. aureus*-infected osteoblasts revealed colonies of dead bacteria bodies that were embedded or surrounded by the mineralized organic matrix (Figures 7d to 7f). The empty vacuoles of the fully degraded bacteria surrounded by the calcium crystal deposits are evident in the ECM region (Figures 7g to 7i). Interestingly, residual intracellular bacteria colony is evident within some host cells. Most of the residual intracellular bacteria showed impaired microstructure, such as damaged cell wall (Figures 7j to 7k). The unstimulated RMP-treated *S. aureus*-infected osteoblasts revealed no calcium crystal deposits within the ECM (Figure 7l).

Comparable expression levels of major bone formation genes in the RMP-treated *S. aureus*-infected osteoblasts and uninfected RMP-treated osteoblasts. To further assess the osteogenic competence of the *S. aureus*-infected osteoblasts after treatment with multiple doses of 8 µg/ml RMP, the gene expression levels of prominent bone formation markers were assessed via quantitative polymerase chain reaction (qPCR) at days 7, 14, and 21 of osteogenesis. To explore the direct effect of the intracellular bacterial infection on matrix mineralization, the RMP-treated *S. aureus*-infected osteoblasts were compared to the corresponding RMP-treated uninfected control group. The results as presented in Figure 8 show no significant difference in the expression of the master transcription gene runt-related transcription factor 2 (*RUNX2*). Furthermore, comparable levels were seen in the gene expression of collagen type 1 (*COL1A1*), bone morphogenic protein type 2 (*BMP-2*), alkaline phosphatase, biomineralization associated (*ALPL*), secreted protein acidic and rich in cysteine (*SPARC*), bone gamma-carboxyglutamate protein/osteocalcin (*BGLAP*), tumour necrosis factor (TNF) receptor super-family member 11b/osteoprotegerin (*OPG*), and *RANKL*, important cytokines directly involved in bone formation at all three study timepoints. However, the comparison of the RMP-treated *S. aureus*-infected osteoblasts with the untreated native osteoblasts showed a significantly higher expression level of some genes, namely *RUNX2* ($p = 0.018$), *ALPL* ($p = 0.045$), *OPG* ($p = 0.048$), and *RANKL* ($p = 0.037$, all two-way ANOVA) at different stages of osteogenesis.

Discussion

Herein, we investigated the metabolic and osteogenic competence of *S. aureus*-infected osteoblasts after antibiotic therapy. Regarding cellular metabolism, low dose of RMP therapy significantly reduced the intracellular *S. aureus* burden and enabled restoration of the host cell metabolism. Our finding supports previous reports on the potent penetration ability of RMP that enabled substantial eradication of the intracellular bacteria.[21,32,43]

The balanced activity of osteoblasts and osteoclasts is important for maintaining proper homeostasis of bone turnover, and an imbalance would lead to bone loss. *S. aureus* infections can stimulate such changes via induction of inflammatory responses, resulting in bone destruction. High expression of inflammatory cytokines leads to a shift in bone turnover by increasing the differentiation of

osteoclasts and diminishing osteoblast-mediated matrix production and mineralization, ultimately resulting in bone destruction.[44] The human osteoblast-like Saos-2 cells are suitable for studying in vitro osteogenesis due to their ability to produce ample mineralized matrix.[45,46] Hence, Saos-2 cells were used to investigate the osteogenic competence of the *S. aureus*-infected osteoblasts after multiple RMP therapy. In comparison to the uninfected control groups, the RMP-treated infected osteoblasts deposited a significantly lower amount of mineralized matrix at seven days of osteogenesis, suggesting that the early osteogenic power of the osteoblasts has been impaired by the intracellular bacterial burden. However, an extended osteogenic stimulation with RMP treatment up to 21 days produced significantly higher amounts of mineralized extracellular organic matrix. This shows that prolonged osteogenic stimulation coupled with antibiotic therapy facilitates deposition of improved extracellular mineralized organic matrix.

Conversely, 21 days osteogenic stimulation of the *S. aureus*-infected osteoblasts without RMP treatment revealed no form of organic matrix formation and mineralization, and significantly reduced ALP activity at both the early and later stages of osteogenesis due to the destruction and lysis of osteoblasts by the high intracellular bacteria burden. Reduction in osteoblast proliferation, ECM formation, and mineralization was observed when mouse clonal MC3T3-E1 pre-osteoblastic cell line was infected with formaldehyde-fixed *S. aureus* strains with overexpression of SpA, Panton-Valentine leukocidin (PVL), and coagulase (Coa) proteins.[31,47] This indicates that major virulence factors of *S. aureus* can impair osteoblast proliferation, bone matrix formation, and mineralization, which can be regained after antibiotic therapy.

Another important novel finding of this study supporting the organic matrix formation and mineralization competence of the RMP-treated infected osteoblasts following 21 days of osteogenesis is the abundant organic and inorganic extracellular components evident at the ultrastructural level. The ultrastructure analysis revealed viable osteoblasts that were surrounded by a densely mineralized ECM. The mineral deposits appeared as dense needle-like calcium crystals that integrated with the organic matrix. The empty vacuoles of fully degraded bacteria indicate high efficacy of low-dose RMP therapy, and the ability of osteoblasts to use their cellular machinery bodies to efficiently degrade and dispose of dead bacteria bodies. However, the presence of residual bodies of damaged bacteria within the mineralized extracellular and intracellular compartments even after prolonged RMP therapy indicates that complete eradication of intracellular bacteria is difficult, as evident in chronic osteomyelitis patients.[18] The embedding of the damaged bacteria bodies within the mineralized ECM could possibly delay treatment time, and the densely mineralized organic matrix could potentially act as a safe residence for any viable antibiotic-resistant bacteria strains, which if not fully eradicated can lead to recurrent infection.

The positive osteogenic competence of the infected osteoblasts following RMP therapy is also evident at the gene level. Differentiation into mature osteoblasts is governed by the transcriptional factor *RUNX2*.[48] During osteogenesis, *RUNX2* stimulates the expression of specific ECM proteins such as *COL1A1, ALP, BGLAP,* and *SPARC*.[49,50] The similar expression levels of these genes, as seen in infected and uninfected RMP-treated groups, indicate that the RMP therapy positively impacted their matrix formation and mineralization functions. Past reports on staphylococcal osteomyelitis have shown significant downregulation of *OPG* levels in infected osteoblasts.[36,51] Besides stimulating bone formation, osteoblasts regulate bone resorption via an indirect control of osteoclast activation and differentiation through the *RANKL/OPG* pathway. Thus, the comparable expression levels of *OPG,* and the *RANKL/OPG* ratio evident in the RMP-treated infected and uninfected groups, imply a positive influence of the RMP therapy. However, the significantly higher expression of *RUNX2, ALPL,* and *OPG* in the untreated native osteoblasts shows the inherent osteoblastic phenotype of the Saos-2 cells, or possibly suggests that multiple-antibiotic treatment might interfere with the expression levels of certain genes at different stages of osteogenesis.

In conclusion, the findings of this in vitro study show that intracellular *S. aureus* infection can substantially impair osteoblast metabolism and function. However, treatment with a potent intracellular penetrating antibiotic at reduced concentration can restore the metabolic and osteogenic competence of surviving osteoblasts. Delay in early osteogenesis caused by the intracellular bacterial burden can be greatly improved at later osteogenesis.

Our study highlights the positive effect of intracellular bacteria clearance on bone matrix formation and mineralization level. Further, in vivo and clinical investigation are needed to understand the role of *S. aureus* and its virulence factors in the impairment of osteoblast functions, particularly metabolism, bone matrix formation, and the mineralization process.

References

1. **Alt V**, **Rupp M**, **Langer M**, **Baumann F**, **Trampuz A**. Infographic: can the oncology classification system be used for prosthetic joint infection?: the PJI-TNM system. *Bone Joint Res.* 2020;9(2):77–78.
2. **Alt V**, **Rupp M**, **Langer M**, **Baumann F**, **Trampuz A**. Can the oncology classification system be used for prosthetic joint infection?: the PJI-TNM system. *Bone Joint Res.* 2020;9(2):79–81.
3. **Ellington JK**, **Harris M**, **Hudson MC**, **Vishin S**, **Webb LX**, **Sherertz R**. Intracellular Staphylococcus aureus and antibiotic resistance: implications for treatment of staphylococcal osteomyelitis. *J Orthop Res.* 2006;24(1):87–93.
4. **Urish KL**, **Cassat JE**. Staphylococcus aureus osteomyelitis: bone, bugs, and surgery. *Infect Immun.* 2020;88(7):e00932-19.
5. **Kremers HM**, **Nwojo ME**, **Ransom JE**, **Wood-Wentz CM**, **Melton LJ**, **Huddleston PM**. Trends in the epidemiology of osteomyelitis: a population-based study, 1969 to 2009. *J Bone Joint Surg Am.* 2015;97-A(10):837–845.
6. **Lew DP**, **Waldvogel FA**. Osteomyelitis. *N Engl J Med.* 1997;336(14):999–1007.

7. **Peltola H**, **Pääkkönen M**. Acute osteomyelitis in children. *N Engl J Med*. 2014;370(4):352–360.
8. **Raina DB**, **Liu Y**, **Jacobson OLP**, **Tanner KE**, **Tägil M**, **Lidgren L**. Bone mineral as a drug-seeking moiety and a waste dump. *Bone Joint Res*. 2020;9(10):709–718.
9. **Pijls BG**, **Sanders IMJG**, **Kujiper EJ**, **Nelissen RGHH**. Induction heating for eradicating *Staphylococcus epidermidis* from biofilm. *Bone Joint Res*. 2020;9(4):192–199.
10. **Milstrey A**, **Rosslenbroich S**, **Everding J**, **et al**. Antibiofilm efficacy of focused high-energy extracorporeal shockwaves and antibiotics in vitro. *Bone Joint Res*. 2021;10(1):77–84.
11. **Horn J**, **Stelzner K**, **Rudel T**, **Fraunholz M**. Inside job: staphylococcus aureus host-pathogen interactions. *Int J Med Microbiol*. 2018;308(6):607–624.
12. **Hudson MC**, **Ramp WK**, **Nicholson NC**, **Williams AS**, **Nousiainen MT**. Internalization of Staphylococcus aureus by cultured osteoblasts. *Microb Pathog*. 1995;19(6):409–419.
13. **Moldovan A**, **Fraunholz MJ**. In or out: Phagosomal escape of Staphylococcus aureus. *Cell Microbiol*. 2019;21(3):e12997.
14. **de Mesy Bentley KL**, **Trombetta R**, **Nishitani K**, **et al**. Evidence of Staphylococcus aureus deformation, proliferation, and migration in canaliculi of live cortical bone in murine models of osteomyelitis. *J Bone Miner Res*. 2017;32(5):985–990.
15. **Zoller SD**, **Hegde V**, **Burke ZDC**, **et al**. Evading the host response: Staphylococcus "hiding" in cortical bone canalicular system causes increased bacterial burden. *Bone Res*. 2020;8(1):43.
16. **Krauss JL**, **Roper PM**, **Ballard A**, **et al**. Staphylococcus aureus infects osteoclasts and replicates intracellularly. *mBio*. 2019;10(5):e02447-19.
17. **Yang D**, **Wijenayaka AR**, **Solomon LB**, **et al**. Novel insights into Staphylococcus aureus deep bone infections: the involvement of osteocytes. *mBio*. 2018;9(2):e00415-18.
18. **Walter N**, **Mendelsohn D**, **Brochhausen C**, **Rupp M**, **Alt V**. Intracellular S. aureus in osteoblasts in a clinical sample from a patient with chronic osteomyelitis - a case report. *Pathogens*. 2021;10(8):1064.
19. **Sinha B**, **Fraunholz M**. Staphylococcus aureus host cell invasion and post-invasion events. *Int J Med Microbiol*. 2010;300(2–3):170–175.
20. **Tuchscherr L**, **Heitmann V**, **Hussain M**, **et al**. Staphylococcus aureus small-colony variants are adapted phenotypes for intracellular persistence. *J Infect Dis*. 2010;202(7):1031–1040.
21. **Yu K**, **Song L**, **Kang HP**, **Kwon H-K**, **Back J**, **Lee FY**. Recalcitrant methicillin-resistant *Staphylococcus aureus* infection of bone cells: Intracellular penetration and control strategies. *Bone Joint Res*. 2020;9(2):49–59.
22. **Gao T**, **Lin J**, **Zhang C**, **Zhu H**, **Zheng X**. Is intracellular *Staphylococcus aureus* associated with recurrent infection in a rat model of open fracture? *Bone Joint Res*. 2020;9(2):71–76.
23. **Ahmed S**, **Meghji S**, **Williams RJ**, **Henderson B**, **Brock JH**, **Nair SP**. Staphylococcus aureus fibronectin binding proteins are essential for internalization by osteoblasts but do not account for differences in intracellular levels of bacteria. *Infect Immun*. 2001;69(5):2872–2877.
24. **Foster TJ**. The MSCRAMM family of cell-wall-anchored surface proteins of gram-positive cocci. *Trends Microbiol*. 2019;27(11):927–941.
25. **Elasri MO**, **Thomas JR**, **Skinner RA**, **et al**. Staphylococcus aureus collagen adhesin contributes to the pathogenesis of osteomyelitis. *Bone*. 2002;30(1):275–280.
26. **Rydén C**, **Yacoub AI**, **Maxe I**, **et al**. Specific binding of bone sialoprotein to Staphylococcus aureus isolated from patients with osteomyelitis. *Eur J Biochem*. 1989;184(2):331–336.
27. **Claro T**, **Widaa A**, **McDonnell C**, **Foster TJ**, **O'Brien FJ**, **Kerrigan SW**. Staphylococcus aureus protein A binding to osteoblast tumour necrosis factor receptor 1 results in activation of nuclear factor kappa B and release of interleukin-6 in bone infection. *Microbiology*. 2013;159(Pt 1):147–154.
28. **Reilly SS**, **Hudson MC**, **Kellam JF**, **Ramp WK**. In vivo internalization of Staphylococcus aureus by embryonic chick osteoblasts. *Bone*. 2000;26(1):63–70.
29. **Alexander EH**, **Rivera FA**, **Marriott I**, **Anguita J**, **Bost KL**, **Hudson MC**. Staphylococcus aureus - induced tumor necrosis factor - related apoptosis - inducing ligand expression mediates apoptosis and caspase-8 activation in infected osteoblasts. *BMC Microbiol*. 2003;3:5.
30. **Tucker KA**, **Reilly SS**, **Leslie CS**, **Hudson MC**. Intracellular Staphylococcus aureus induces apoptosis in mouse osteoblasts. *FEMS Microbiol Lett*. 2000;186(2):151–156.
31. **Jin T**, **Zhu YL**, **Li J**, **et al**. Staphylococcal protein A, Panton-Valentine leukocidin and coagulase aggravate the bone loss and bone destruction in osteomyelitis. *Cell Physiol Biochem*. 2013;32(2):322–333.
32. **Mohamed W**, **Sommer U**, **Sethi S**, **et al**. Intracellular proliferation of S. aureus in osteoblasts and effects of rifampicin and gentamicin on S. aureus intracellular proliferation and survival. *Eur Cell Mater*. 2014;28:258–268.
33. **Boyle WJ**, **Simonet WS**, **Lacey DL**. Osteoclast differentiation and activation. *Nature*. 2003;423(6937):337–342.
34. **Kong YY**, **Yoshida H**, **Sarosi I**, **et al**. OPGL is a key regulator of osteoclastogenesis, lymphocyte development and lymph-node organogenesis. *Nature*. 1999;397(6717):315–323.
35. **Claro T**, **Widaa A**, **O'Seaghdha M**, **et al**. Staphylococcus aureus protein A binds to osteoblasts and triggers signals that weaken bone in osteomyelitis. *PLoS One*. 2011;6(4):e18748.
36. **Young AB**, **Cooley ID**, **Chauhan VS**, **Marriott I**. Causative agents of osteomyelitis induce death domain-containing TNF-related apoptosis-inducing ligand receptor expression on osteoblasts. *Bone*. 2011;48(4):857–863.
37. **Kreis CA**, **Raschke MJ**, **Roßlenbroich SB**, **Tholema-Hans N**, **Löffler B**, **Fuchs T**. Therapy of intracellular Staphylococcus aureus by tigecyclin. *BMC Infect Dis*. 2013;13(1):267.
38. **Valour F**, **Trouillet-Assant S**, **Riffard N**, **et al**. Antimicrobial activity against intraosteoblastic Staphylococcus aureus. *Antimicrob Agents Chemother*. 2015;59(4):2029–2036.
39. **Alt V**, **Bitschnau A**, **Osterling J**, **et al**. The effects of combined gentamicin-hydroxyapatite coating for cementless joint prostheses on the reduction of infection rates in a rabbit infection prophylaxis model. *Biomaterials*. 2006;27(26):4627–4634.
40. **Chen JL**, **Steele TWJ**, **Stuckey DC**. Metabolic reduction of resazurin; location within the cell for cytotoxicity assays. *Biotechnol Bioeng*. 2018;115(2):351–358.
41. **O'Brien J**, **Wilson I**, **Orton T**, **Pognan F**. Investigation of the Alamar Blue (resazurin) fluorescent dye for the assessment of mammalian cell cytotoxicity. *Eur J Biochem*. 2000;267(17):5421–5426.
42. **Docheva D**, **Padula D**, **Popov C**, **et al**. Establishment of immortalized periodontal ligament progenitor cell line and its behavioural analysis on smooth and rough titanium surface. *Eur Cell Mater*. 2010;19:228–241.
43. **Thabit AK**, **Fatani DF**, **Bamakhrama MS**, **Barnawi OA**, **Basudan LO**, **Alhejaili SF**. Antibiotic penetration into bone and joints: an updated review. *Int J Infect Dis*. 2019;81:128–136.
44. **Wright JA**, **Nair SP**. Interaction of staphylococci with bone. *Int J Med Microbiol*. 2010;300(2–3):193–204.
45. **Fedde KN**. Human osteosarcoma cells spontaneously release matrix-vesicle-like structures with the capacity to mineralize. *Bone Miner*. 1992;17(2):145–151.
46. **McQuillan DJ**, **Richardson MD**, **Bateman JF**. Matrix deposition by a calcifying human osteogenic sarcoma cell line (SAOS-2). *Bone*. 1995;16(4):415–426.
47. **Widaa A**, **Claro T**, **Foster TJ**, **O'Brien FJ**, **Kerrigan SW**. Staphylococcus aureus protein A plays a critical role in mediating bone destruction and bone loss in osteomyelitis. *PLoS One*. 2012;7(7):e40586.
48. **Komori T**. Regulation of osteoblast differentiation by Runx2. *Adv Exp Med Biol*. 2010;658:43–49.
49. **Komori T**. Regulation of bone development and extracellular matrix protein genes by RUNX2. *Cell Tissue Res*. 2010;339(1):189–195.
50. **Stein GS**, **Lian JB**, **van Wijnen AJ**, **et al**. Runx2 control of organization, assembly and activity of the regulatory machinery for skeletal gene expression. *Oncogene*. 2004;23(24):4315–4329.
51. **Somayaji SN**, **Ritchie S**, **Sahraei M**, **Marriott I**, **Hudson MC**. Staphylococcus aureus induces expression of receptor activator of NF-kappaB ligand and prostaglandin E2 in infected murine osteoblasts. *Infect Immun*. 2008;76(11):5120–5126.

Author information:

- F. I. Alagboso, PhD, Research Fellow
- G. K. Mannala, PhD, Research Fellow
  Laboratory for Experimental Trauma Surgery, Department of Trauma Surgery, University Hospital Regensburg, Regensburg, Germany.
- N. Walter, MSc, Research Fellow
- V. Alt, MD, PhD, Head of Department
- M. Rupp, MD, Orthopaedic Surgeon
  Laboratory for Experimental Trauma Surgery, Department of Trauma Surgery, University Hospital Regensburg, Regensburg, Germany; Department of Trauma Surgery, University Hospital Regensburg, Regensburg, Germany.
- D. Docheva, PhD, Head of Department, Laboratory for Experimental Trauma Surgery, Department of Trauma Surgery, University Hospital Regensburg, Regensburg, Germany; Department of Musculoskeletal Tissue Regeneration, Orthopaedic Hospital Koenig-Ludwig-Haus, University of Wuerzburg, Wuerzburg, Germany.
- C. Brochhausen, MD, Head of Laboratory, Institute of Pathology, University Regensburg, Regensburg, Germany.

Author contributions:
- F. I. Alagboso: Investigation, Methodology, Validation, Data curation, Formal Analysis, Visualization, Writing – original draft, Writing – review & editing.
- G. K. Mannala: Investigation, Methodology, Validation, Data curation, Writing – review & editing.
- N. Walter: Investigation, Writing – review & editing.
- D. Docheva: Investigation, Methodology, Supervision, Writing – review & editing.
- C. Brochhausen: Investigation, Methodology, Visualization, Writing – review & editing.
- V. Alt: Conceptualization, Funding acquisition, Supervision, Resources, Writing – review & editing.
- M. Rupp: Conceptualization, Funding acquisition, Supervision, Resources, Writing – review & editing.

Funding statement:
- The authors disclose receipt of the following financial or material support for the research, authorship, and/or publication of this article: open access funding for the manuscript from the open access scheme of University Library of Regensburg.

ICMJE COI statement:
- The authors declare that this research work was performed in the absence of any commercial or financial relationship that could be interpreted as a potential conflict of interest.

Data sharing:
- Data are available upon request through the corresponding author.

Acknowledgements:
- The authors thank Ruth Schewior and Tobias Gsottberger from the Laboratory for Experimental Trauma Surgery, University Clinic, Regensburg and Heiko Siegmund from the Institute of Pathology, University of Regensburg for their valuable technical assistance. Also, the authors thank Dr. Sara Steinmann from the Laboratory for Experimental Trauma Surgery, University Clinic, Regensburg for performing the quantitative polymerase chain reaction (qPCR) analysis. The authors would like to thank Prof. Gessner group for support during this work.

Open access funding
- The authors report that they received open access funding for their manuscript from the open access scheme of University Library of Regensburg.

© 2022 Author(s) et al. This is an open-access article distributed under the terms of the Creative Commons Attribution Non-Commercial No Derivatives (CC BY-NC-ND 4.0) licence, which permits the copying and redistribution of the work only, and provided the original author and source are credited. See https://creativecommons.org/licenses/by-nc-nd/4.0/